Designing Dual-State and Aggregation-Induced Emissive Luminogens from Lignocellulosic Biosourced Molecules

Maelys Bonnot , Nagahm Ibrahim , Magali Allain , Pierre Frère *

Posted Date: 5 June 2024

doi: 10.20944/preprints202406.0318.v1

Keywords: cyanostilbene derivatives; dual-state emission; bio-sourced materials; fluorescence emission

 doi:10.20944/preprints202406.0318.v1

Article

Designing Dual-State and Aggregation-Induced Emissive Luminogens from Lignocellulosic Biosourced Molecules

Maelys Bonnot, Nagham Ibrahim, Magali Allain and Pierre Frère *

UNIV Angers, CNRS UMR 6200 MOLTECH-Anjou, 2 Boulevard Lavoisier 49000 Angers, France
* Correspondence: pierre.frere@univ-angers.fr

Abstract: Utilizing lignocellulosic biosourced platforms, we synthesized novel cyanostilbene (CS) derivatives featuring the 3,4-dimethoxyphenyl moiety. These derivatives were investigated for their emission properties in both solution and solid states. The two simple CS derivatives exhibit very weak luminescence in solution but significant luminescence in the solid state, indicating distinct Aggregation-Induced Emission (AIE) characteristic. Furthermore, combining these two CS units, without conjugation and with quasi perpendicular orientation, results in Dual-State Emission (DSE) fluorophore showing luminescence both in solution and solid states. X-ray crystallography studies on the solid-state compounds reveal a structure-emission relationship, demonstrating that the colour emission correlates with the conformations adopted by the molecules in the solid state, which influence the type of stacking.

Keywords: cyanostilbene derivatives; dual-state emission; bio-sourced materials; fluorescence emission

1. Introduction

In the field of organic fluorophores, the design of molecular structures plays a pivotal role in achieving efficient emission, whether in dilute solutions or within aggregates, powders, and crystals [1,2]. Rigorous -conjugated derivatives often exhibit high luminescence in diluted solutions, with emission color strongly influenced by molecular structural factors like -extension and intramolecular donor-acceptor charge transfer. However, many of these molecules experience a significant reduction or even quenching of their emission as concentration increases, leading to aggregate formation driven by non-radiative deactivation pathways such as cofacial π–π stacking and the presence of trap states. Beyond these conjugated molecules, often termed ACQ derivatives due to their aggregation-induced quenching behavior, a diverse array of purely organic compounds exhibits an opposing effect, characterized by solid-state luminescence enhancement (SLE) or aggregation-induced emission (AIE).[3–6] Lastly, a third category of luminescent derivatives, known as dual-state emission (DSE), possesses the unique attribute of luminescing both in solution and in the solid state [7–12].

While the majority of conjugated systems are synthesized using raw materials sourced from fossil resources, the incorporation of biomass-derived units into these systems is currently emerging in order to find ways allowing to produce sustainable materials that have a lower environmental impact [13,14]. Biomass feedstocks, such as agricultural residues and wood chips, constitute an inexpensive renewable resource for commercial large-scale biorefineries, as these waste products are widely available and can sequester carbon. Among the different biosourced platforms [15], lignocellulosic biomass, mainly composed of cellulose, hemicellulose and lignin [16], offer the advantage of remarkably short production cycles, often less than five years, and hold the potential to yield a diverse array of polyfunctional aromatic molecules, such as furaldehydes and hydroxybenzaldehydes [17] that can be highly relevant for the creation of specialized conjugated

 doi:10.20944/preprints202406.0318.v1

systems [18,19]. Furaldehyde derivatives, such as methylfurfural and hydroxymethylfurfural (HMF), are derived from cellulose [20], while lignin, enables the extraction of phenol derivatives such as vanillin or analogs [21–24].

In our ongoing projects that delve into harnessing biosourced molecules derived from plants and the development of compounds with extended π-conjugation for electronic properties and luminescence [25–27], we introduce here a novel series of cyanostilbene (CS) derivatives integrating 3,4-dimethoxyphenyl and furan units, capitalizing on biosourced raw materials such as vanillin and HMF (Figure 1) [28,29]. α-Cyanostilbene derivatives are highly attractive luminescent materials in the solid state with photophysical properties which are modulated both by the diversity and structural flexibility of the molecules and by the types of stacking of the molecules that generate the solid [28–32]. Most compounds of the CS family exhibit an AIE effect with much greater luminescence in the solid state than in solution. However, through strategic design modifications of CS derivatives, recent synthesis efforts have yielded several compounds that demonstrate varying levels of emission in solution [33–39]. We showcase how uncomplicated structural modifications empower us to craft compounds with remarkably diverse luminescent characteristics, spanning from low-emission systems to those exhibiting AIE or DSE behavior. Furthermore, the use of Knoevenagel condensation to generate cyanovinyl bonds, a sustainable and green reaction occurring under mild conditions without generating toxic byproducts, enables the exploration of luminescent material development within the framework of sustainable development.

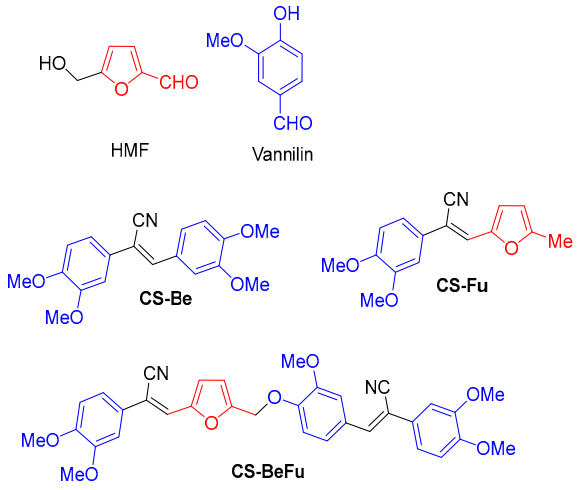

Figure 1. Biosourced molecules HMF and Vannilin and structures of the synthesized cyanostilbene luminophores **CS-Be**, **CS-Fu** and **CS-BeFu**.

2. Results and Discussion

2.1. Synthesis

All the compounds were synthesized in the last step by a Knoevenagel reaction involving the benzyl cyanide derivatives **1**, easily obtained in two steps from vanillyl alcohol.[40] The Knoevenagel condensations for obtaining the compounds **CS-Be** and **CS-Fu** from the benzylcyanide **1** with the corresponding aldehydes 3,4-dimethoxybenzaldehyde and methylfurfural were easily carried out in ethanol at room temperature in presence of catalytic amount of tBuONa (Scheme 1). The obtained precipitates were filtered and washed with ethanol to give **CS-Be** and **CS-Fu** in 85 % and 65% yields respectively.

Preprints.org (www.preprints.org) | NOT PEER-REVIEWED | Posted: 5 June 2024 doi:10.20944/preprints202406.0318.v1

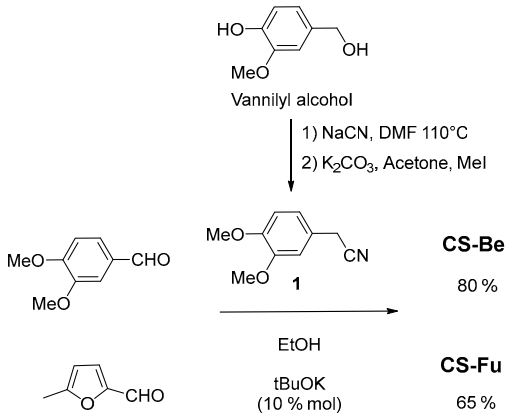

Scheme 1. Knoevenagel condensation with the benzyl cyanide 1.

The dialdehyde derivative **BeFu** integrating both benzaldehyde and furaldehyde units has been synthesized from vanillin and hydroxymethylfuraldehyde (**HMF**) (Scheme 2). Treatment of **HMF** solution in dichloroethane with concentrated bromydric acid (48%) at room temperature leads to bromine derivative **BrMF** in 80 % yield. The green oil obtained after the usual works up, was directly engaged in a Williamson reaction with vanillin to afford the dialdehyde **BeFu** in 80 % yield. The biscondensation of Knoevenagel between dialdehyde **BeFu** and a slight excess of three equivalents of benzylcyanide **1** were carried out in a mixture of tetrahydrofurane (THF) and ethanol (5/10 vv) at 50 °C in presence of 10 % mol of tBuONa during 15 min. After cooling at 0°C, a precipitate slowly appeared to give after filtration target molecules **CS-BeFu** in 55 % yield.

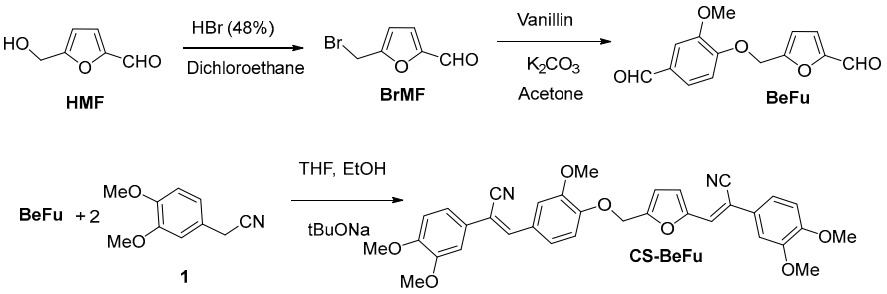

Scheme 2. Synthesis of dialdehydes **BeFu** and biscyanostilbene derivatives **CS-BuFu.**

The ^{1}H NMR of **CS-Be** and **CS-Fu** in $CDCl_3$ are characterized by the presence of only one singlet corresponding to the signal of the vinylic proton. Moreover, an exact number of carbons was observed in the ^{13} C NMR spectra of all the compounds. These NMR results provide sound evidence that only one configurational vinylene isomer in each solid sample. For **Cs-BeFu**, the ^{1}H NMR in DMSO d_6 (Figure S1 in the supporting information) shows that the two ethylenic protons have the same chemical shift at 7.91 ppm and all aromatic protons are well defined, as expected if each ethylenic bond only exists in one configuration. Single-crystals of the three compounds, enabling the characterization by X-ray diffraction have been obtained, thus allowing to unequivocally confirm the Z-configurations of the cyanovinyl bonds in each structure (Figure S2 in the supporting information).

2.2. Electronic Properties

The electronic properties of the molecules were evaluated by theoretical calculation performed at the ab initio density functional level using the Gaussian09 package. Becke's three parameter gradient corrected functional (B3LYP) with a polarized 6.311G(d,p) was used for the geometrical optimization and for the HOMO and LUMO level determination. The Z-configuration for the cyanovinyl units was used for the calculation for all the compounds. The Figure 2 shows the representation of the HOMO and LUMO levels and indicates the energy levels of the three compounds. For both compounds **CS-Be** and **CS-Fu**, the HOMO exhibits delocalization over the

Preprints.org (www.preprints.org) | NOT PEER-REVIEWED | Posted: 5 June 2024 doi:10.20944/preprints202406.0318.v1

entire conjugated system, while the LUMO is more localized on the central cyanovinyl bond. While the energy levels of the LUMO are very close for **CS-Be** and **CS-Fu**, the energy level of the HOMO for **CS-Fu** is destabilized compared to that of **CS-Be**, indicating a more electron-donating character of the methylfuran group than the 3,4-dimethoxyphenyl group. Consequently, the HOMO-LUMO gap is slightly lower for **CS-Fu** than for **CS-Be**. Geometrical optimization for the **CS-BeFu** molecule reveals that the two CS units named *Cs-Fu* and *Cs-Be* lie in two nearly perpendicular planes. Energy calculations lead to very close HOMO and HOMO-1 levels, with HOMO-1 localized on the *Cs-Fu* part and HOMO on *Cs-Be*. Similarly, the close LUMO and LUMO+1 levels respectively show localization on the *Cs-Fu* and C*s-Be* parts. Overall, the respective gaps for each of the two parts *Cs-Fu* (HOMO-1 - LUMO) and *Cs-Be* (HOMO - LUMO+1) are lower than those calculated for the **CS-Fu** and **CS-Be** molecules.

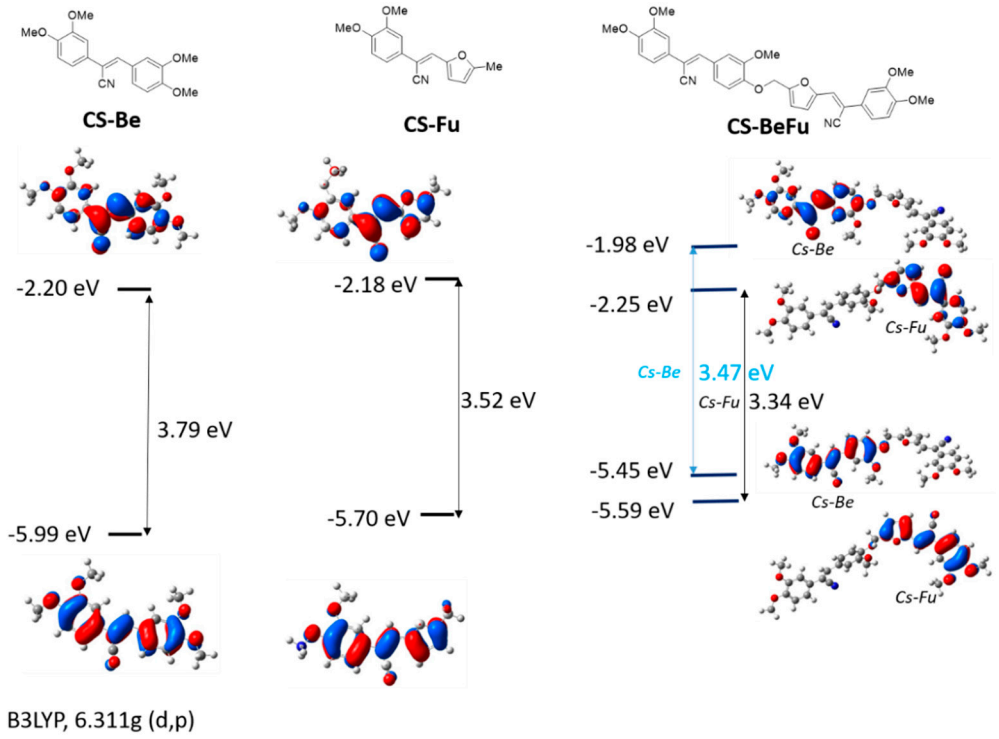

Figure 2. HOMO and LUMO frontier orbitals along with their corresponding enegy levels calculated by gas phase DFT.

2.3. Optical Data

The UV-Vis absorption and fluorescence were performed in dilute (10^{-5} M) cyclohexane solution, then the fluorescence was also measured in the solid state. For the fluorescence, the quantum yields **Φ** correspond to the absolute values obtained from an integrated sphere. All the data are gathered in Table 1.

Table 1. This is a table. Tables should be placed in the main text near to the first time they are cited.

	CS-Be	**CS-Fu**	**CS-BeFu**
	Solution [1]		
λ_{abs} (nm)	352	354	358
ε (mol $L^{-1}cm^{-1}$)	23000	25600	33000
ΔE_{opt} (eV) [2]	3.03	2.95	2.91
$\lambda_{em\text{-}solu}$ (nm)	426	453	457
Φ_{solu} (%) [3]	<1	<1	15
ΔE_{rot} (kJ/mol) [4]	19	20	39

 doi:10.20944/preprints202406.0318.v1

	Solid [5]		
$\lambda_{em\text{-}solid}$ (nm)	450	527	476 538
Φ_{solid} (%) [3]	46	5	25
$\Delta\lambda_{emi}$ (eV) [6]	0.16	0.38	0.41
ΔE_{cou} (eV) [7]	0.21	0.38	0.20 0.30
τ (ns)	2.3 (85.4 %) 4.6 (14.6 %)	2.2 (71.0 %) 5.1 (29.0 %)	1.9 (12.4 %) 4.3 (45.7 %) 7.2 (41.9 %)
τ_{aver} (ns)	2.6	3.1	5.2
k_r (ns^{-1}) [8]	0.177	0.016	0.048
k_{nr} (ns^{-1}) [9]	0.21	0.31	0.14

[1] 10^{-5} M in cyclohexane. [2] calculated from the foot of the absorption band. [3] Absolute emission quantum yield measured with an integrating sphere. [4] Obtained from the TD-DFT calculation. [5] Measurements performed for the crystals. [6] $\Delta\lambda_{emi} = \lambda_{em\text{-}solu} - \lambda_{emi\text{-}solid}$. [7] $\Delta E_{cou} = S_{1mono} - S_{1dimer}$. [8] Radiative rate constants, calculated according to $k_r = \Phi/\tau_{aver}$. [h] Non-radiative rate constants, calculated by $\tau_{aver}^{-1} = k_r + k_{nr}$.

2.3.1. Optical Properties in Solution

The UV-Vis absorption and emission spectrums are presented in the Figure 3a. The UV-Vis absorption spectra of **CS-Be** and **CS-Fu** present a band around 350 nm corresponding to the HOMO-LUMO transitions with a band gap about 3.0 eV. The presence of two independent CS units in **CS-BeFu** leads to a larger band and an increase of the molar absorption coefficient. Under excitation at 350 nm, **CS-Be** and **CS-Fu** present a low blue emission in solution in cyclohexane with a quantum yields that do not exceed 1%. For the compound **CS-BeFu** the emission is higher with the quantum yield that reaches Φ_{solu}= 15%.

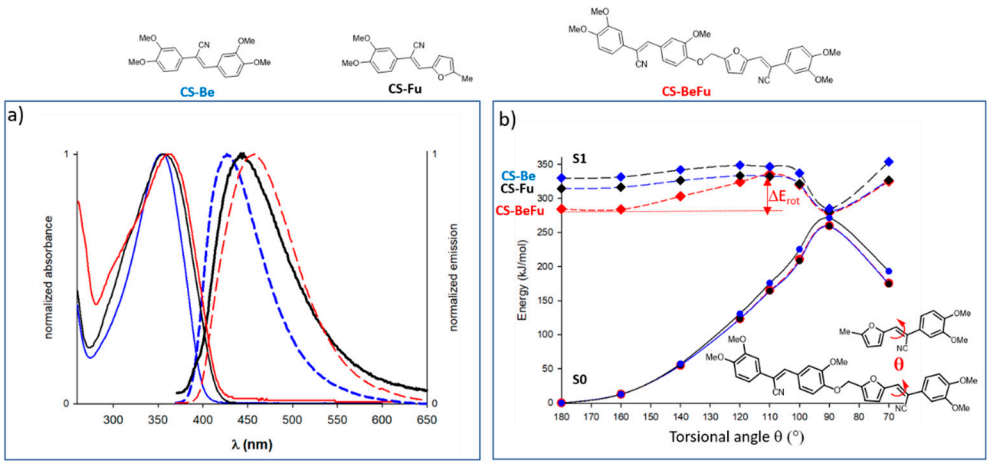

Figure 3. a) Normalized UV-Vis absorption (lines) and emission (dotted lines) in 10^{-5} M solution in cyclohexane of **CS-Be** (blue), **CS-Fu** (black) and **CS-BeFu** (red). b) TD-DFT torsional scans of double bonds θ for **CS-Be** (blue), **CS-Fu** (black) and **CS-BeFu** (red) using the optimized S_0 state at the TD-B3LYP/6.31G(d,p) level, S_0 and S_1 energies were computed for each data point.

Many cyanostilbene (CS) compounds typically show minimal or no luminescence when dissolved and exposed to irradiation [29]. This fluorescence quenching is often attributed to the steric effect of the cyano group, which triggers the unrestricted rotation of aromatic units around the vinyl group, leading to elevated non-radiative rates. To assess the possibility of luminescence in solution for dicyanostilbene-type derivatives, J. Gierschner et al. propose that the excited Franck-Condon (FC) state energy can evolve with torsion of the double bond to reach the conical intersection (CI) corresponding to a minimum energy of the S_1 level that is very close to the maximum level reached

 doi:10.20944/preprints202406.0318.v1

for S_0 [41–43]. Effective access to the CI, for a 90° torsion of the ethylenic bond, from the FC state energy can be achieved through a rotation barrier (ΔE_{rot}). A low ΔE_{rot} value will increase the probability of de-excitation by internal conversion and thus inhibit luminescence. Conversely, an increase in ΔE_{rot} via a stabilisation of the FC state, can inhibit effective access to the CI and thus enhance luminescence in solution. To demonstrate access to the CI and calculate ΔE_{rot} values for the **Cs-Be**, **CS-Fu**, and **CS-BeFu** compounds, TD-DFT calculations were performed to estimate the energies of the S_1 and S_0 states, following rotation around the cyanovinyl bond with angles θ ranging from 180 to 70° [39]. For the **CS-BeFu** compound, calculations were performed considering the bond of the Fu part. Theoretical calculations were performed considering the B3LYP/6-31G (d,p) basis set and cyclohexane as the solvent. Although TD-DFT is not an appropriate method to describe the region at the CI, nevertheless TD-DFT is considered to be sufficiently good to describe the path toward the SI [42]. The results for each compound are presented in Figures S3–S5 in the supporting information. The three compounds show a CI state at θ = 90° with a minimum energy of the S_1 state close to the maximum energy obtained for the S_0 state. The access to the CI state from the S_1 energy at the Franck-Condon state (θ = 180°) can determinate internal conversion possibility which would be responsible of the non-radiative decay. As shown in Figure 3b, the stabilization of the FC state for the compound **CS-BeFu** leading to a rotation barrier ΔE_{rot} = 39 kJ/mol at the S_1 state is higher than for **CS-Fu and CS-Be** at 20 kJ/mol. This result reveals that the access to CI is more difficult for **CS-BeFu** and does not allow IC and consequently justifying the fluorescence of **CS-BeFu** in solution.

2.3.2. Emission in the Solid State for the Crystals

The three compounds present a more or less emission in the solid state (Figure 4). The spectra of **CS-Be** is characterized by an unstructured band with maxima at wavelengths of 426 nm and show a quantum yield of 46%, corresponding to a strong emission in the blue. The compound **CS-Fu** exhibit more structured emission bands with the appearance of shoulders and a maximum at 527 nm, corresponding to a yellow emission. However, **CS-Fu** is very weakly emissive with a quantum yield of only 5%.

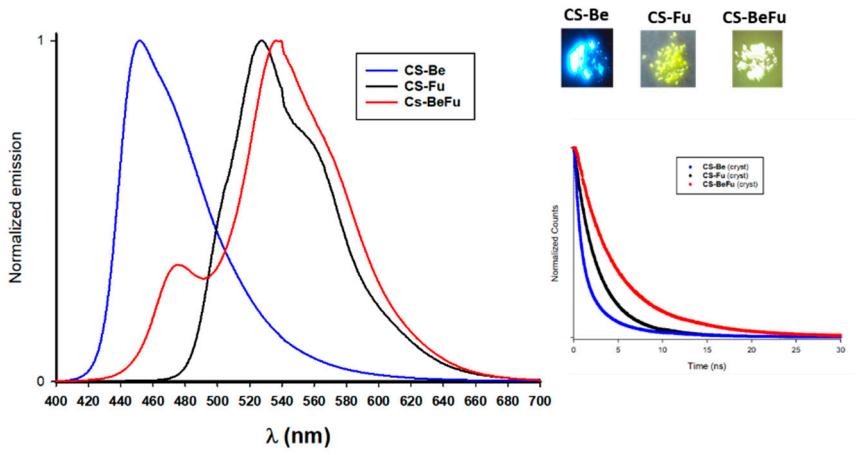

Figure 4. Normalized emission spectra for the crystals of **CS-Be** (blue), **CS-Fu** (black) and **CS-BeFu** (red) under λ_{exc} = 350 nm. Photograph of emission under excitation at 350 nm. Fluorescence lifetime for crystals of **CS-Be** (blue), **CS-Fu** (black) and **CS-BeFu** (red).

For the compound **CS-BeFu**, which can be considered as a combination of **CS-Be** and **CS-Fu**, it is interesting to note that the emission spectrum, characterized by a small band peaking at 476 nm and a more intense band with a maximum at 538 nm, closely resembles that of **CS-Fu** but with a higher quantum yield of 25%, leading to a well perceptible yellow emission. Fluorescence lifetimes for the crystals range from 2.6 ns for **CS-Be** to 5.3 ns for **CS-BeFu**. The electronic properties of the CS compounds being very similar, it is evidently the molecular assembly rather than the molecular structure that can explain the significant differences in the observed photophysical properties of the crystals [1,44,45]. Having the X-ray structures of **CS-Be**, **CS-Fu** and **CS-BeFu**, it was possible to

 doi:10.20944/preprints202406.0318.v1

analyze the structure-property relationships of these three compounds which present very different emissions for their crystals

2.4. Structure Property Relationships

The structure of **CS-Be** (Figure 5a), exhibit a packing mode characterized by a head-to-tail stacking of molecules along the a-axis, with the dimethoxyphenyl-C=CN unit (in red in Figure 7) overlapping the other dimethoxyphenyl unit. However, due to significant torsion in the molecule, the dihedral angle between the two planes defined by the phenyl rings is 53.5°, There is not any π–π stacking and the shorter interatomic distances between overlapping molecules is d_1 = 3.48 Å (blue dotted line in Figure 5a). Between adjacent stacking columns, numerous hydrogen bonding interactions occur, involving the nitrogen atoms of the cyano group and the ethylenic hydrogen (highlighted in orange in Figure 7), as well as the oxygen and hydrogen atoms of the methoxy groups (highlighted in green in Figure 5).

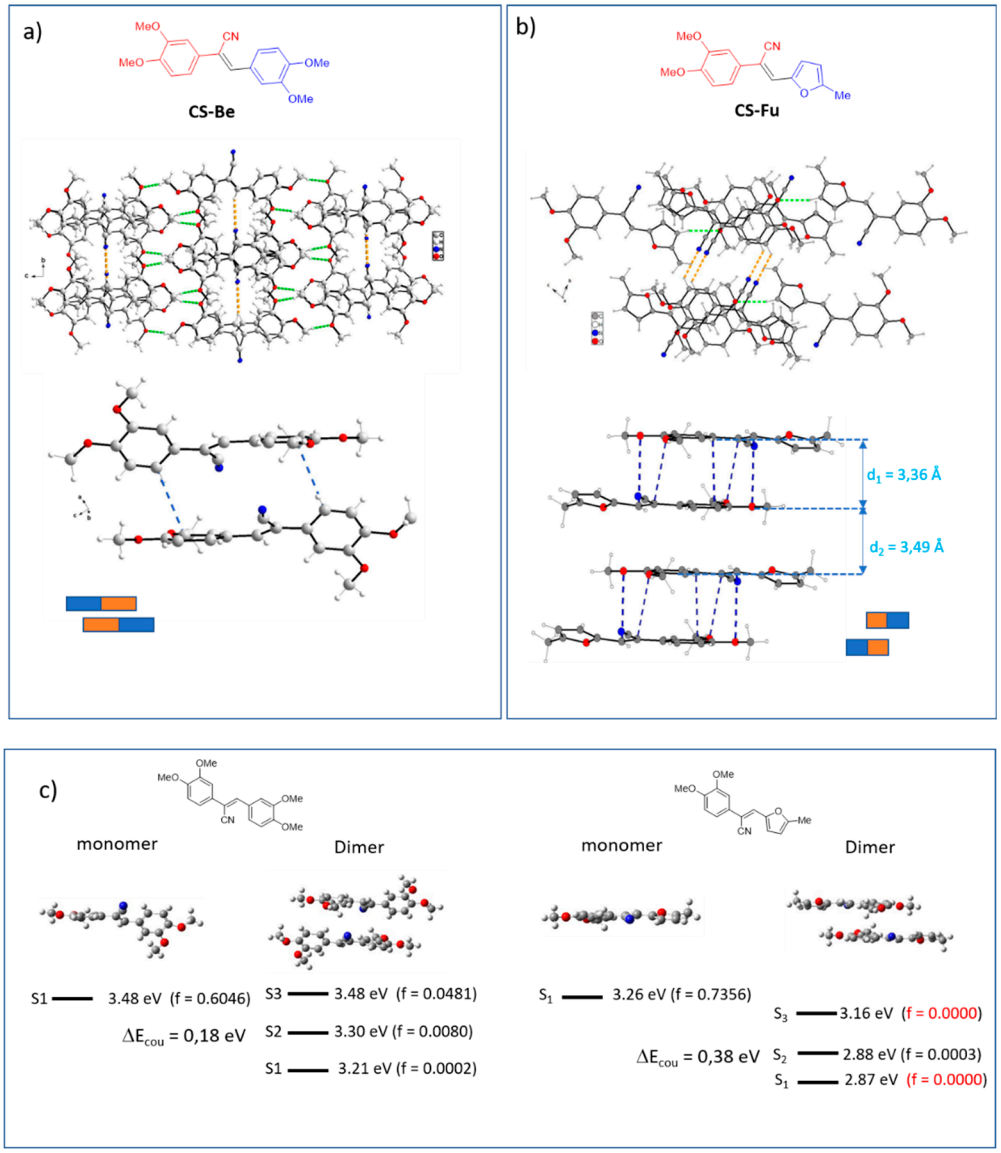

Figure 5. Packing modes of the molecules in crystals. a) **CS-Be**, b) **CS-Fu**. Hydrogen bonds involving the nitrogen atoms are in orange dotted lines, those involving the oxygen atoms in green dotted lines and the short C---C intermolecular distances are in blue dotted lines. c) The calculated vertical transition energies of **CS-Be** and **CS-Fu** in the nearest-neighbor configurations according to the single crystal X-ray structures. Energies of the first singlet excited states S1-S3 (oscillator strength in parenthesis).

 doi:10.20944/preprints202406.0318.v1

For the well different structure of **CS-Fu** (Figure 5b), the nearly planar molecules, featuring a dihedral angle of 20.2° between their two aromatic rings, stack along the a-axis, forming closely contacting dimers. The distances between the planes defined by the phenyl rings and the ethylenic bond are d_1 = 3.36 Å and d_2 = 3.49 Å, signifying robust π interactions within **CS-Fu** crystals. These interactions give rise to numerous intermolecular distances with d_{C-C} values less than 3.5 Å.

These significantly different stacking modes account for the substantial variation in emissions between the two compounds. On one hand, inter-column interactions through multiple hydrogen bonds in **CS-Be** contribute significantly to limit vibrational and intramolecular motion (RIM) within the solids [3]. The relatively weak π interactions favor each molecule's contribution as an emissive species with very low excitonic coupling. For compound **CS-Fu**, the formation of dimers with stronger π interactions leads to a significant decrease in luminescence, resulting in a shift towards yellow, indicative of excitonic-type emission. To explore the correlation between the molecular arrangement and the luminescence in the solid state, time-dependent density functional theory (TD-DFT, B3LYP/6.31g (d,p)) calculations were performed with Gaussian 09 by using the classical dimer approach [1]. Monomers and dimers subtracted from each crystal were used for the calculations. The results are presented in the Figure 5c. For the **CS-Be** dimer, the TD-DFT calculations give a level S_1 with a very weak oscillator force *f* then higher levels with more substantial oscillator forces. The excitonic coupling considering the S_2 level is 0.18 eV. We can therefore consider that in the crystal, it is the monomers which act as the emissive species to dissipate the excitation energy by radiative transitions in the blue. Conversely for the **CS-Fu** compound, the calculations give null or extremely weak oscillator forces for the first excited states and the excitonic coupling of 0.38 eV is much larger. This result which well considers the π–π interactions between the molecules agrees with the formation of excimer leading to a weak emission with a shift of the emission into the yellow. The difference between the fluorescence lifetimes for the two crystals also argues for these different types of emission. **CS-Fu** exhibits a longer fluorescence lifetime than that of **CS-Be**, as expected for an excimer emission in **CS-Fu** [46,47].

Considering the X-Ray structure of **CS-BeFu** presented in Figure 6a, the two cyanostilbene units, denoted *Cs-Fu* and *Cs-Be* are in almost perpendicular planes and they pile up independently along two directions. The only interactions between the two CS units are via hydrogen bonds between the nitrogen atom of the *Cs-Fu* unit and an aromatic hydrogen atom of the 3,4-dimethoxyphenyl group of the *Cs-Be* unit. The stacking of *Cs-Fu* units is carried out with strong contacts involving furan units (green dotted line in Figure 6) with a distance separating the planes defined by the furans d_2= 3.37 Å. On the other hand, between the *Cs-Be* units, there are few contacts and these are weaker, the distance between the planes of the internal phenyl rings is d_1= 3.54 Å. For the calculations, both types of dimers were considered (Figure 6b). Interactions between *Cs-Fu* units give excited states with non-zero oscillator strengths and an excitonic coupling of 0.30 eV. Between the *Cs-Be* units, the excitonic coupling of 0.20 eV is weaker. These results are compatible with obtaining a broad band presenting both an emission in the yellow of the excimeric type which could be due to the *Cs-Fu* part and another in the blue of the excitonic type for the *Cs-Be* part.

Preprints.org (www.preprints.org) | NOT PEER-REVIEWED | Posted: 5 June 2024 doi:10.20944/preprints202406.0318.v1

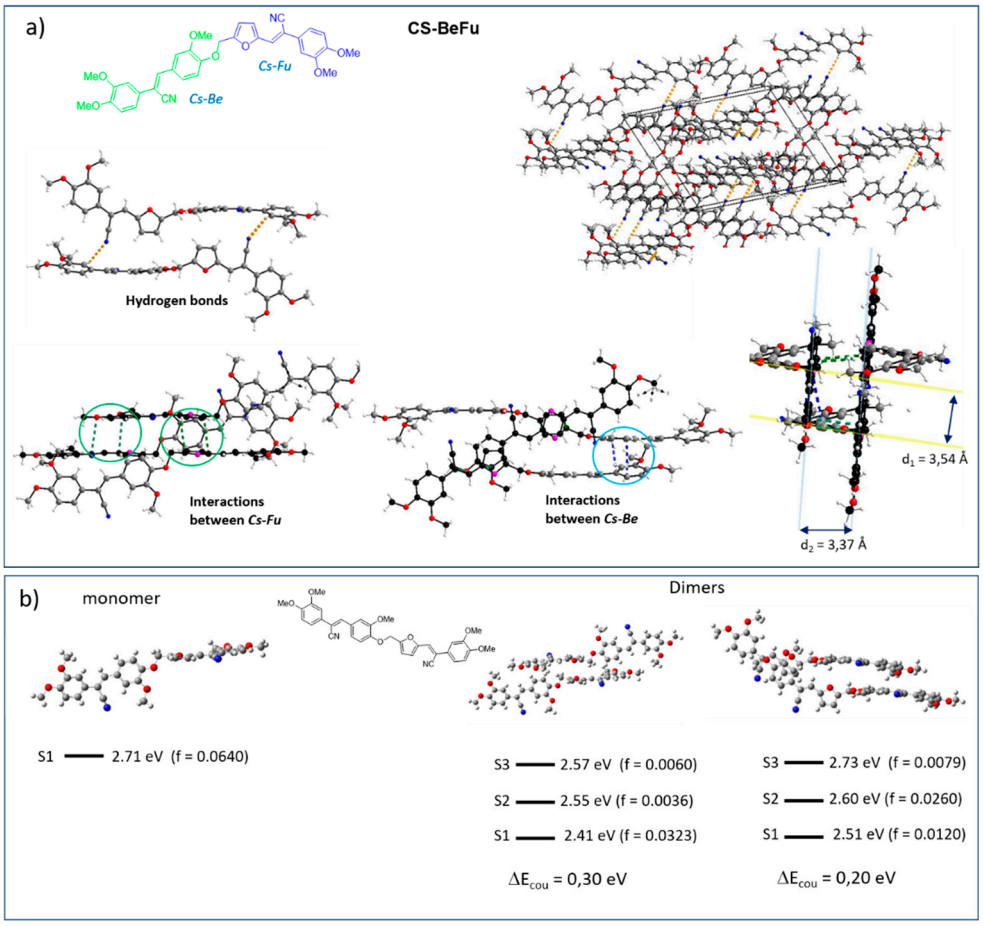

Figure 6. a) X-ray structure of CS-BeFu showing the intermolecular interactions. b) The calculated vertical transition energies for the *Cs-Be* and *Cs-Fu* part in the nearest-neighbor configurations according to the single crystal X-ray structure of **CS-BeFu**. Energies of the first singlet excited states S1-S3 (oscillator strength in parenthesis).

3. Conclusion

By utilizing biosourced molecules from the lignocellulose platform, such as vanillin and 5-hydroxymethylfurfural, we have developed derivatives from the cyanostilbene family that exhibit specific luminescent properties in both solution and solid states. The Knoevenagel condensation between 3,4-dimethoxyphenyl acetonitrile and either 5-methylfurfural or 3,4-dimethoxybenzaldehyde results in two cyanostilbene units, CS-Fu and CS-Be, which demonstrate an Aggregation-Induced Emission (AIE) effect with very low emission in solution and significantly higher emission in the solid state. However, when these two CS units are linked without conjugation by a methyleneoxy bridge, creating a nearly perpendicular arrangement of the two conjugated CS arms in the molecule CS-BeFu, a luminescent compound with a Dual-State Emission (DSE) effect is obtained, characterized by similar luminescence in both solution and crystalline states. The increase in luminescence in solution is explained by a decrease in the energy of the Franck-Condon excited state for CS-BeFu compared to the individual Cs-Fu and Cs-Be units, which require more energy to overcome the activation energy barrier to reach the energy of the conical intersection of the S_1 state.

Furthermore, the significantly different emissions in the crystals, both in terms of wavelengths and quantum yields, ranging from the intense blue-green for the CS-Be compound to the low-intensity yellow for CS-Fu, with an intermediate yellow-orange emission for CS-BeFu, are explained by the considerable differences in the stacking modes of the molecules in the crystals. The weak π interactions observed in the crystals of the CS-Be compound induce an excitonic type emission, whereas the strong π interactions in CS-Fu favour a much weaker excimeric type emission that is red-shifted. For CS-BeFu, the existence of independent interactions between the two perpendicularly

 doi:10.20944/preprints202406.0318.v1

oriented CS arms, with few π interactions for *Cs-Be* and more numerous ones for *Cs-Fu*, results in an emission characterized by a very broad emission spectrum.

4. Experimental Section

4.1. Materials and Methods

UV-Vis and Fluorescent Spectroscopy

Absorption spectra were recorded on a Shimadzu UV-1800 spectrophotometer. Fluorescent emission spectra were obtained on a FP-8500 spectrofluorometer. The fluorescence quantum yields both in solution and in the solid state were measured using an ILF-835 | 100 mm Integrating Sphere.

X-Ray Analysing

Crystal data were collected on a Rigaku Oxford SuperNova diffractometer equipped with an Atlas CCD detector and micro-focus Cu-K_α radiation (λ = 1.54184 Å). The structures were solved by dual-space algorithm and refined on F^2 by full matrix least-squares techniques using SHELX package (G.M. Sheldrick, ShelXT2018/2, ShelXL2018/3-2019/3). All non-hydrogen atoms were refined anisotropically and the H atoms were included in the calculation without refinement. Multiscan empirical absorption was corrected by using CrysAlisPro program (CrysAlisPro, Agilent Technologies, 2020-2021).

CCDC numbers of all the structures (see Table S1 in the SI) contain the supplementary crystallographic data for this paper. These data are provided free of charge by the joint Cambridge Crystallographic Data Centre and Fachinformationszentrum Karlsruhe Access Structures service. www.ccdc.cam.ac.uk/structures.

4.2. Syntheses and Characterization of Compounds

*Synthesis of **BeFu***

To a solution of **HMF** (0.5 g, 4 mmol) in 10 ml of DCM, 5 ml of 48% HBr is added. The mixture is left stirring at room temperature for 12 h, then is washed with a saturated solution of sodium hydrogen carbonate then with water. After drying the organic phase and evaporation of the solvent, a green oil (0.57 g) is obtained corresponding exclusively to 5-bromomethylfuraldehyde **BrMF** verified by NMR (Yield = 75%).

BrMF (0.57 g, 3 mmol) is directly used for the Williamson reaction with 1.2 equivalents of vanillin (0.55 g, 3.6 mmol) and 3 equivalents of K_2CO_3 (1.24 g, 9 mmol) in 50 ml of acetone. After refluxing for 12 hours, the solid suspension is removed by filtration and the filtrate is evaporated under vacuum. The residue is purified by chromatography on silica, eluting DCM/AcOEt (8/2) to give the dialdehyde **BeFu** with a yield of 70%.

***BrMF** : ^{1}H NMR ($CDCl_3$): 9.63 (s, 1H), 7.19 (d, 1H, J = 3.6 Hz), 6.58 (d, 1H, J = 3.6 Hz), 4.49 (s, 2H).*

***BeFu** : ^{1}H NMR ($CDCl_3$): δ 9.87 (s, 1H), 9.65 (s, 1H), 7.45 – 7.43 (m, 2H), 7.24 (d, 1H, J = 3.6 Hz), 7.05 (d, 1H, J = 8.7 Hz), 6.66 (d, 1H, J = 3.6 Hz), 5.23 (s, 2H), 3.94 (s, 3H).*

Procedure for the mono condensation of Knoevenagel

A mixture of aldehyde (4 mmol), acetonitrile derivative (4.4 mmol) and a catalytic amount of ^{t}BuONa (0.4 mmol) was let in ethanol without stirring (10 mL) for 6 h at room temperature in dark. The resulting precipitate was filtered, washed with cold ethanol. Afterwards, it was dried in high vacuo to give the targeted compounds in crystalline state.

*(Z)-2,3-bis(3,4-dimethoxyphenyl)acrylonitrile **CS-Be***

Colorless crystalline powders (80% yield). M.p.155°C. ^{1}H NMR (300 MHz, $CDCl_3$) δ 7.67 (d, 2H, J = Hz), 7.36 (s, 1H), 7.37-7.34 (dd, *J* = 8.4 Hz, *J* = 2.2 Hz 1H), 7.26-7.22 (dd, *J* = 8.4 Hz, *J* = 2.2 Hz 1H)

 doi:10.20944/preprints202406.0318.v1

7.12 (d, *J* = 2.2 Hz, 1H), 7.13 (d, 2H, J = 2.2 Hz), 6.93 (d, *J* = 8.4 Hz, 1H), 6.91 (d, *J* = 8.4 Hz, 1H), 3.97 (s, 3H), 3.96 (s, 3H), 3.95 (s, 3H), 3.93 (s, 3H). ^{13}C NMR (75 MHz, $CDCl_3$) δ 150.9, 149.8, 149.3, 149.0, 140.5, 127.7, 126.9, 124.0, 118.8, 111.3, 111.0, 110.7, 109.7, 108.7, 108.6, 57.0, 56.0, 55.0. Anal. calcd. (%) for $C_{19}H_{19}NO_4$: C,70.14; H,5.89; N,4.31. Found (%): C,70.23; H,5.80; N,4.45.

(Z)-2-(3,4-dimethoxyphenyl)-3-(5-methylfuran-2-yl)acrylonitrile ***CS-Fu***

Yellow crystalline powders (65% yield). M.p.108°C. ^{1}H NMR (300 MHz, $CDCl_3$) δ, 7.22-7.19 (dd, *J* = 8.4 Hz, *J* = 2.0 Hz, 1H), 7.20 (s, 1H), 7.09 (d, J = 2.2 Hz, 1H) , 7.07 (d, J = 3.4 Hz , 1H), 6.89 (d, J= 8.4 Hz), 6.19 (d, *J* = 3.4 Hz, 1H), 3.94 (s, 3H), 3.91 (s, 3H), 2.40 (s, 3H). ^{13}C NMR (75 MHz, $CDCl_3$) δ 155.3, 149.6, 149.2, 148.9, 126.8, 126.4, 118.5, 118.2, 116.2, 111.3, 109.5, 109.4, 108.0, 105.3, 56.0, 14.0. Anal. calcd. (%) for $C_{16}H_{15}NO_3$: C,71.36; H,5.61; N,5.20. Found (%): C,71.44; H,5.69; N,5.24.

Synthesis of ***CS-BeFu***

To a solution of dialdehyde **BeFu** (520 mg, 2 mmol) in 5 mL of THF at 50 °C was added the 3,4-dimethoxyphenylacetonitrile **1** (531 mg, 3 mmol) dissolved in 10 mL of ethanol then 20 mg of ^{t}BuONa. The solution was stirred at 50°C during 15 min, then the mixture was let down at 0°C to see for obtaining a precipitation. The solid was filtered, washed with cold ethanol then dried in vacuo.

Yellow crystalline powders (45% yield). M.p.350°C. ^{1}H NMR (300 MHz, DMSO-d_6) δ 7.91 (s, 2H), 7.66 (d, 1H, J= 2.1 Hz), 7.58 (dd, 1H, J = 8.7 Hz, J = 2.1 Hz), 7.39-7.33 (m, 3H), 7.28-7.24 (m, 2H), 7.17 (d, 1H, J = 3.6 Hz), 7.09 (dd, 2H, J = 8.7 Hz, J = 2.1 Hz), 6.93 (d, 1H, J= 3.6 Hz), 5.29 (s, 2H), 3.88 (s, 3H), 3.87 (s, 3H), 3.84 (s, 3H), 3.83 and 3.82 (2s, 6H). ^{13}C NMR : Solubility too low. HRMS m/z calculated for $C_{34}H_{30}N_2O_7Na$: 601.1951; found: 601.1955.

Supplementary Materials: The following supporting information can be downloaded at the website of this paper posted on Preprints.org.

References

1. Gierschner, J.; Shi, J.; Milián-Medina, B.; Roca-Sanjuán, D.; Varghese, S.; Park, S., Luminescence in Crystalline Organic Materials: From Molecules to Molecular Solids. *Adv. Opt. Mater.* **2021,** 9, 2002251.
2. Mei, J.; Leung, N. L. C.; Kwok, R. T. K.; Lam, J. W. Y.; Tang, B. Z., Aggregation-Induced Emission: Together We Shine, United We Soar! *Chem. Rev.* **2015,** 115, 11718-11940.
3. Voskuhl, J.; Giese, M., Mesogens with aggregation-induced emission properties: Materials with a bright future. *Aggregate* **2022,** 3, e124.
4. Würthner, F., Aggregation-Induced Emission (AIE): A Historical Perspective. *Angew. Chem. Int. Ed.* **2020,** 59, 14192-14196.
5. Zhao, Z.; Zhang, H.; Lam, J. W. Y.; Tang, B. Z., Aggregation-Induced Emission: New Vistas at the Aggregate Level. *Angew. Chem. Int. Ed.* **2020,** 59, 9888-9907.
6. Turelli, M.; Ciofini, I.; Wang, Q.; Ottochian, A.; Labat, F.; Adamo, C., Organic compounds for solid state luminescence enhancement/aggregation induced emission: a theoretical perspective. *Phys. Chem. Chem. Phys.* **2023,** 25, 17769-17786.
7. Belmonte-Vázquez, J. L.; Amador-Sánchez, Y. A.; Rodríguez-Cortés, L. A.; Rodríguez-Molina, B., Dual-State Emission (DSE) in Organic Fluorophores: Design and Applications. *Chem. Mater.* **2021,** 33, 7160-7184.
8. Huber, A.; Dubbert, J.; Scherz, T. D.; Voskuhl, J., Design Concepts for Solution and Solid-State Emitters – A Modern Viewpoint on Classical and Non-Classical Approaches. *Chem. Eur. J.* **2023,** 29, e202202481.
9. Rodríguez-Cortés, L. A.; Navarro-Huerta, A.; Rodríguez-Molina, B., One molecule to light it all: The era of dual-state emission. *Matter* **2021,** 4, 2622-2624.
10. Xia, G.; Si, L.; Wang, H., Dual-state emission: the compatible art of substantial rigidity and twisting conformation within a single molecule. *Mater. Today. Chem.* **2023,** 30, 101596.
11. Stoerkler, T.; Pariat, T.; Laurent, A. D.; Jacquemin, D.; Ulrich, G.; Massue, J., Excited-State Intramolecular Proton Transfer Dyes with Dual-State Emission Properties: Concept, Examples and Applications. *Molecules* **2022,** 27.
12. Ma, Z.; Tu, J.; Yang, D.; Zhang, Q.; Wu, J., Recent advances in organic small-molecular dual-state emission probes. *J. Mol. Struct.* **2024,** 1312, 138478.
13. Boivin, L.-P.; Dupont, W.; Gendron, D.; Leclerc, M., Biosourced Monomers: Toward Sustainable Conjugated Polymers for Organic Electronics. *Macromol. Chem.Phys.* **2023,** 224, 2200378.

 doi:10.20944/preprints202406.0318.v1

14. Giraud, L.; Grelier, S.; Grau, E.; Hadziioannou, G.; Brochon, C.; Cramail, H.; Cloutet, E., Upgrading the chemistry of π-conjugated polymers toward more sustainable materials. *J. Mater. Chem. C* **2020,** 8, 9792-9810.
15. Kohli, K.; Prajapati, R.; Sharma, B. K., Bio-Based Chemicals from Renewable Biomass for Integrated Biorefineries. *Energies* **2019,** 12, 233.
16. Wang, Y.; Zhang, Y.; Cui, Q.; Feng, Y.; Xuan, J., Composition of Lignocellulose Hydrolysate in Different Biorefinery Strategies: Nutrients and Inhibitors. *Molecules* **2024,** 29, 2275.
17. Decostanzi, M.; Auvergne, R.; Boutevin, B.; Caillol, S., Biobased phenol and furan derivative coupling for the synthesis of functional monomers. *Green Chem.* **2019,** 21, 724-747.
18. Isikgor, F. H.; Becer, C. R., Lignocellulosic biomass: a sustainable platform for the production of bio-based chemicals and polymers. *Polym. Chem.* **2015,** 6, 4497-4559.
19. Zheng, B.; Huo, L., Recent Advances of Furan and Its Derivatives Based Semiconductor Materials for Organic Photovoltaics. *Small Methods* **2021,** 5, 2100493.
20. Karlinskii, B. Y.; Ananikov, V. P., Recent advances in the development of green furan ring-containing polymeric materials based on renewable plant biomass. *Chem. Soc. Rev.* **2023**.
21. Fache, M.; Boutevin, B.; Caillol, S., Vanillin Production from Lignin and Its Use as a Renewable Chemical. *ACS Sustain. Chem. Eng.* **2016,** 4, 35-46.
22. Xu, L.; Liaqat, F.; Sun, J.; Khazi, M. I.; Xie, R.; Zhu, D., Advances in the vanillin synthesis and biotransformation: A review. *Renew. Sustain. Energy Rev.* **2024,** 189, 113905.
23. Martău, G. A.; Călinoiu, L.-F.; Vodnar, D. C., Bio-vanillin: Towards a sustainable industrial production. *Trends Food Sci. Technol.* **2021,** 109, 579-592.
24. D'Arrigo, P.; Rossato, L. A. M.; Strini, A.; Serra, S., From Waste to Value: Recent Insights into Producing Vanillin from Lignin. *Molecules* **2024,** 29, 442.
25. Mallet, C.; Moussallem, C.; Faurie, A.; Allain, M.; Gohier, F.; Skene, W. G.; Frère, P., Rational Topological Design for Fluorescence Enhancement upon Aggregation of Distyrylfuran Derivatives. *Chem. Eur. J.* **2015,** 21, 7944-7953.
26. Ibrahim, N.; Moussallem, C.; Allain, M.; Segut, O.; Gohier, F.; Frère, P., Exploring the Electronic Properties of Extended Benzofuran-Cyanovinyl Derivatives Obtained from Lignocellulosic and Carbohydrate Platforms Raw Materials. *ChemPlusChem* **2021,** 86, 475-482.
27. Mallet, C.; Frère, P., Furylenevinylene Oligomers as Extended Conjugated Systems from Renewable Materials. *Eur. J; Org. Chem.* **2022,** 2022, e202201276.
28. Gao, A.; Wang, Q.; Wu, H.; Zhao, J.-W.; Cao, X., Research progress on AIE cyanostilbene-based self-assembly gels: Design, regulation and applications. *Coord. Chem. Rev.* **2022,** 471, 214753.
29. Mahalingavelar, P.; Kanvah, S., α-Cyanostilbene: a multifunctional spectral engineering motif. *Phys. Chem. Chem. Phys.* **2022,** 24, 23049-23075.
30. Martínez-Abadía, M.; Giménez, R.; Ros, M. B., Self-Assembled α-Cyanostilbenes for Advanced Functional Materials. *Adv. Mater.* **2018,** 30, 1704161.
31. Zhao, J.; Chi, Z.; Zhang, Y.; Mao, Z.; Yang, Z.; Ubba, E.; Chi, Z., Recent progress in the mechanofluorochromism of cyanoethylene derivatives with aggregation-induced emission. *J. Mater. Chem. C* **2018,** 6, 6327-6353.
32. Lin, S.; Gutierrez-Cuevas, K. G.; Zhang, X.; Guo, J.; Li, Q., Fluorescent Photochromic α-Cyanodiarylethene Molecular Switches: An Emerging and Promising Class of Functional Diarylethene. *Adv. Funct. Mater.* **2021,** 31, 2007957.
33. Wu, H.; Chen, Z.; Chi, W.; Bindra, A. K.; Gu, L.; Qian, C.; Wu, B.; Yue, B.; Liu, G.; Yang, G.; Zhu, L.; Zhao, Y., Structural Engineering of Luminogens with High Emission Efficiency Both in Solution and in the Solid State. *Angew. Chem. Int. Ed.* **2019,** 58, 11419-11423.
34. Huang, Z.; Tang, F.; He, F.; Kong, L.; Huang, J.; Yang, J.; Ding, A., Pyrene and triphenylamine substituted cyanostyrene and cyanostilbene derivatives with dual-state emission for high-contrast mechanofluorochromism and cell imaging. *Org. Chem. Front.* **2022,** 9, 5118-5124.
35. Xue, J.; Tang, F.; Ding, A.; He, F.; Huang, J.; Kong, L.; Yang, J., α-Cyanostilbene functionalized carbazole derivatives exhibiting dual-state emission and multi-stimuli responsive fluorescent switching. *J. Luminescence* **2022,** 250, 119119.
36. Zhu, X.; Feng, L.; Cao, S.; Wang, J.; Niu, G., Donor–Acceptor–Acceptor-Conjugated Dual-State Emissive Acrylonitriles: Investigating the Effect of Acceptor Unit Order and Biological Imaging. *Org. Lett.* **2022**.
37. Ni, Y.; Yang, L.; Kong, L.; Wang, C.; Zhang, Q.; Yang, J., Highly efficient dual-state emission and two-photon absorption of novel naphthalimide functionalized cyanostilbene derivatives with finely tuned terminal alkoxyl groups. *Mater. Chem. Front.* **2022,** 6, 3522-3530.
38. Shi, Q.; Ni, Y.; Yang, L.; Kong, L.; Gu, P.; Wang, C.; Zhang, Q.; Zhou, H.; Yang, J., Fluorination of naphthalimide–cyanostilbene derivatives to achieve dual-state emission luminogens with strong fluorescence in highly polar environments for bioimaging. *J. Mater. Chem. B* **2023,** 11, 6859-6867.

 doi:10.20944/preprints202406.0318.v1

39. Ibrahim, N.; Loumaigne, M.; Grolleau, J.; Allain, M.; Frère, P., Dual-state emission versus no emission by manipulating the molecular structures of cyanovinyl–benzofuran derivatives. *Mol. Syst.. Des. Eng.* **2022**.
40. Schwartz, M. A.; Zoda, M.; Vishnuvajjala, B.; Mami, I., A convenient synthesis of o- and p-hydroxy substituted phenylacetonitriles and phenethylamines. *J. Org. Chem.* **1976,** 41, 2502-2503.
41. Shi, J.; Aguilar Suarez, L. E.; Yoon, S.-J.; Varghese, S.; Serpa, C.; Park, S. Y.; Lüer, L.; Roca-Sanjuán, D.; Milián-Medina, B.; Gierschner, J., Solid State Luminescence Enhancement in π-Conjugated Materials: Unraveling the Mechanism beyond the Framework of AIE/AIEE. *J. Phys. Chem. C* **2017,** 121, 23166-23183.
42. Shi, J.; Izquierdo, M. A.; Oh, S.; Park, S. Y.; Milián-Medina, B.; Roca-Sanjuán, D.; Gierschner, J., Inverted energy gap law for the nonradiative decay in fluorescent floppy molecules: larger fluorescence quantum yields for smaller energy gaps. *Org. Chem. Front.* **2019,** 6, 1948-1954.
43. Rivera, M.; Stojanović, L.; Crespo-Otero, R., Role of Conical Intersections on the Efficiency of Fluorescent Organic Molecular Crystals. *J. Phys. Chem. A* **2021,** 125, 1012-1024.
44. Li, Q.; Li, Z., The Strong Light-Emission Materials in the Aggregated State: What Happens from a Single Molecule to the Collective Group. *Adv. Sci.* **2017,** 4, 1600484.
45. Wang, C.; Li, Z., Molecular conformation and packing: their critical roles in the emission performance of mechanochromic fluorescence materials. *Mater. Chem. Front.* **2017,** 1, 2174-2194.
46. Wilbraham, L.; Louis, M.; Alberga, D.; Brosseau, A.; Guillot, R.; Ito, F.; Labat, F.; Métivier, R.; Allain, C.; Ciofini, I., Revealing the Origins of Mechanically Induced Fluorescence Changes in Organic Molecular Crystals. *Adv. Mater.* **2018,** 30, 1800817.
47. Ding, Z.; Lu, T.; Bi, C.; Li, B.; Zhang, S.-T.; Xu, W.; Jiang, S., A multifunctional material with distinct mechanochromic and piezochromic properties: π-stacking in play. *Mater. Chem. Front.* **2022,** 6, 86-93.